Intrinsic thermal expansivity and hydrational properties of amyloid peptide A B42 in liquid water

ARTICLE *in* THE JOURNAL OF CHEMICAL PHYSICS · DECEMBER 2008

Impact Factor: 2.95 · DOI: 10.1063/1.3012562 · Source: PubMed

5 AUTHORS, INCLUDING:

Ivan V. Brovchenko
Technische Universität Dortmund
92 PUBLICATIONS **1,648** CITATIONS
SEE PROFILE

Alla Oleinikova
Technische Universität Dortmund
91 PUBLICATIONS **2,667** CITATIONS
SEE PROFILE

Intrinsic thermal expansivity and hydrational properties of amyloid peptide $A\beta_{42}$ in liquid water

I. Brovchenko,[a] R. R. Burri, A. Krukau, A. Oleinikova, and R. Winter[b]
Physical Chemistry, Dortmund University of Technology, Otto-Hahn-Str. 6, Dortmund D-44227, Germany

(Received 8 February 2008; accepted 13 October 2008; published online 17 November 2008)

Volumetric and conformational properties of the amyloid $\beta(1-42)$ peptide ($A\beta_{42}$) are studied in relation to the properties of hydration water in a wide temperature range by computer simulations. The apparent volume of $A\beta_{42}$, which is the change in the total volume of the solution due to the presence of $A\beta_{42}$, shows a quite different temperature dependence below and above $T \approx 320$ K. The apparent thermal expansion coefficient $\alpha^{app}(A\beta_{42})$ is about 1.5×10^{-3} K^{-1} at $T \leq 320$ K and about 0.6×10^{-3} K^{-1} at $T > 320$ K. By evaluation of the thermal expansivity of hydration water, the intrinsic expansivity of the biomolecule in liquid water was determined for the first time. The intrinsic thermal expansion coefficient of $A\beta_{42}$ is found to be *negative*: $\alpha^{int}(A\beta_{42}) \approx -0.8 \times 10^{-3}$ K^{-1}. The negative thermal expansion coefficient of $A\beta_{42}$ can be attributed to its rubberlike (entropic) elasticity and/or to a decreasing number of intrapeptide hydrogen bonds. Upon heating, $A\beta_{42}$ transforms from an extended chain with a significant content of α-helices to a compact coil with noticeable content of β-structures. A hydrogen-bonded spanning network of hydration water envelops $A\beta_{42}$ homogeneously at low temperatures but breaks into an ensemble of small water clusters upon heating via a percolation transition, whose midpoint is close to the temperature, where the apparent volume of $A\beta_{42}$ changes its temperature behavior. The mutual relation between the volumetric properties of $A\beta_{42}$, its conformational properties, and the properties of the hydration water is discussed. © *2008 American Institute of Physics*. [DOI: 10.1063/1.3012562]

I. INTRODUCTION

The conformation of a biomolecule may be characterized by various properties, such as its secondary structure, radius of gyration, and volume. Some properties may change gradually, and some other change sharply when crossing a temperature-induced conformational transition. As it is not clear in advance which property is the most adequate order parameter of this transition, it is important to find parameters most sensitive to the conformational changes of a biomolecule. The volume of a biomolecule and its thermal expansivity may be among those properties, which are highly sensitive to conformational transitions.[1] Pressure perturbation calorimetric experimental studies of staphylococcal nuclease (SNase),[2,3] amino acids,[4] and elastinlike peptides[5] show that the apparent thermal expansion coefficient α^{app} of the biomolecules is about $+10^{-4}$ to $+10^{-3}$ K^{-1}. Below the temperature of unfolding, α^{app} typically decreases upon heating. At this temperature, the behavior of α^{app} changes qualitatively, and it may show a minimum, become constant, or even slightly increase upon further heating. The apparent volume of a biomolecule as well as its apparent thermal expansion coefficient include contributions from the biomolecule itself (intrinsic part) and from the hydration water. We may expect that the conformational properties of a biomolecule may be reflected in the volumetric properties of both the biomolecule and its hydration water. An attempt to extract the intrinsic thermal expansivity of a biomolecule in liquid water from experimental data[6] suffers from the lack of information about the temperature dependence of the density of hydration water. Obtaining such information will open the possibility of determining the intrinsic volume of the biomolecule and of analyzing its properties.

Current experimental techniques do not allow estimations of the temperature behavior of the density of hydration water not only near biomolecules but even near extended smooth surfaces, and this situation will presumably persist in the long term perspective.[7] Therefore, computer simulations (computer experiment) and a subsequent analysis of the results on the basis of the theory of surface behavior of fluids[8,9] remain the main sources of information about the thermodynamic properties of fluids near surfaces in general and of the hydration water in particular. It is important to note that the temperature behavior of Lennard-Jones fluids[9] and of water[7,8] near various surfaces seen in simulations is highly universal and closely follows the general theoretical expectations.[10] This evidences the reliability of the results obtained by simulations of fluids near surfaces and the possibility of using them in the analysis of the intrinsic thermodynamic properties of biomolecules. In the present paper, we report to the best of our knowledge the first estimation of the intrinsic thermal expansivity of a biomolecule in liquid water.

To study the mutual relation between the volumetric and conformational properties of a biomolecule and the properties of water in its hydration shell, we have chosen the amyloid peptide $\beta(1-42)$ ($A\beta_{42}$ hereafter). This peptide is one of the major components of amyloid plaques, the hallmark of

[a]Electronic mail: brov@heineken.chemie.uni-dortmund.de.
[b]Electronic mail: roland.winter@tu-dortmund.de.

Alzheimer's disease. Many devastating diseases are directly related to the formation of ordered peptide aggregates.[11,12] In some organic solvents (trifluoroethanol and hexafluoroisopropanol),[13–17] $A\beta_{42}$ is soluble and has a predominantly α-helical conformation. Upon addition of water, the solubility of $A\beta_{42}$ decreases drastically (the upper limit of the critical concentration in water is in the low micromolar range[18]) and the formation of fibril aggregates complicates the analysis of the secondary structure of an isolated $A\beta_{42}$ peptide. Circular dichroism (CD) and NMR studies evidence mainly a disordered structure of $A\beta_{42}$ in water with noticeable content of β-sheets and only a small amount of α-helices.[13–17,19] Presumably, this reflects the structure of the peptide in a partially aggregated state, whereas the conformation of a single $A\beta_{42}$ peptide in water is not very clear. Other $A\beta$ peptides exhibit a similar conformational behavior in water and in apolar solvents.[20]

Higher solubilities of some of the $A\beta$ peptides allowed studies of the concentration and temperature dependence of their secondary structure and approached the monomeric state more closely. The $A\beta(1-40)$ peptide shows temperature-induced changes in the CD spectra upon heating from 0 to 37 °C, which evidence an increasing β-structure content.[21] These changes do not depend on the peptide concentration and, therefore, may be attributed to the properties of the monomer. The peptides $A\beta(10-35)$ (Ref. 22) and $A\beta(1-28)$ (Ref. 23) show a collapsed coil structure in water, and an extensive β-sheet structure appears upon aggregation only. A decrease in the $A\beta(25-35)$ peptide concentration causes a decrease in β-sheet structure (presumably due to the suppression of aggregation) and facilitates disordered structures and β-turns, which may reflect the conformation of a single peptide in water.[24] A similar behavior was reported for $A\beta(11-25)$.[25] The conformation of a single $A\beta_{42}$ peptide[17,26–31] as well as of other $A\beta$ peptides[32–35] in water was intensively studied by molecular dynamics computer simulations. Typically, coil structures dominate the $A\beta$ peptide structure, and to some extent β-sheets and α-helices were also seen. The temperature-induced changes in the conformation of a single $A\beta_{42}$ peptide were studied using simplified interparticle potentials and an implicit solvent:[36] the α-helical content decreases and the β-strand content increases upon heating, in agreement with experimental findings.[21] Fully atomistic simulations of $A\beta$ peptides in explicit water were not implemented yet to study their temperature-induced conformational changes.

Clustering of water molecules in the hydration shell of a biomolecule seems to be closely related to its conformational behavior.[37–40] For example, polymorphic transitions of DNA from the A-form to the biologically relevant B-form occurs close to the hydration level, where a spanning H-bonded water network forms at the DNA surface via a percolation transition.[38,39] At full hydration, this spanning network breaks upon heating at some temperature. For fully hydrated SNase and elastinlike peptides, this break occurs approximately at temperatures where these molecules undergo conformational transitions.[37,40] Besides, we cannot exclude that the expansivity of hydration water may be affected by this percolation transition. Therefore, water clustering in the hydration shell of the biomolecule is an important factor, which should be taken into account when considering the temperature dependence of the conformational and volumetric properties of a biomolecule in liquid water.

In the present paper, we study the volumetric and conformational properties of the $A\beta_{42}$ peptide in liquid water in a wide temperature range. The secondary structure and other structural characteristics of $A\beta_{42}$ are analyzed as functions of temperature. The intrinsic thermal expansion coefficient of $A\beta_{42}$ is estimated by taking into account the expansivity of hydration water. Analysis of water clustering in the hydration shell is used to characterize the thermal breaking of the spanning H-bonded water network. Finally, we discuss the mutual relation between the conformational behavior of $A\beta_{42}$, the thermal expansivities of $A\beta_{42}$ and its hydration water, and the clustering in the hydration water shell.

II. METHODS

The $A\beta_{42}$ peptide in a full stretched conformation (PDB ID 1z0q) (Ref. 17) was placed in a cubic box with 7704 water molecules, and 1000 steps of the steepest descent energy minimization were performed. The GROMACS software package[41] was used with the OPLS force field[42] for the $A\beta_{42}$ peptide and the extended simple point charge (SPCE) model for water. Electroneutrality of $A\beta_{42}$, which initially had a charge of $-3e$, was provided by distributing the neutralizing charge $+3e$ over all $A\beta_{42}$ atoms proportionally to the absolute values of their charges. The sum of the absolute values of the partial charges of 627 atoms of $A\beta_{42}$ is $149.28e$. Therefore, to provide electroneutrality of $A\beta_{42}$, the partial charge of each atom has been increased by about 2% of its initial absolute value. In particular, the partial charge of the amide nitrogen increases from $-0.50e$ to $-0.49e$. Such procedure has negligible effect on the ability of the force field to reproduce the system properties and provides the electroneutrality of the system without adding the counterions, which may affect the hydration water noticeably. A spherical cutoff of 9 Å was used for the short-range intermolecular interactions; the long-range Coulombic interactions were taken into account by particle mesh Ewald summation. Molecular dynamics simulations were performed in the *NPT* ensemble at a constant pressure $P=1$ bar and 22 temperatures between 250 and 460 K using the Nose–Hoover thermostat and the Parrinello–Rahman barostat. Periodic boundary conditions were applied. Simulation runs were performed with 2 fs time steps, and the configuration was saved every 0.1 ps. At each temperature, the system was equilibrated during 1 ns and the subsequent 20 ns run was used for the analysis. Besides, three temperature (280, 340, and 400 K) simulations were prolonged up to 40 ns.

To determine the volume of the $A\beta_{42}$ peptide in aqueous solution, we performed *NPT* simulations of liquid water with the same number ($N=7704$) of water molecules but without $A\beta_{42}$ in the simulation box. The difference between the volumes of the two simulation boxes (with and without $A\beta_{42}$) was considered the apparent volume $V^{app}(A\beta_{42})$ of $A\beta_{42}$. The water density in the first hydration shell was calculated by counting those N_w water molecules, whose oxygen are

situated closer than some distance D to the nearest heavy atom of $A\beta_{42}$. The volume of the hydration water shell was estimated using the solvent accessible surface area (SASA), obtained with a probe radius of 1.4 Å.

To characterize the conformation of the $A\beta_{42}$ peptide, we calculated its radius of gyration R_{gyr}, the SASA, the intrapeptide hydrogen bonds, and their distribution along the peptide chain. The secondary structure was determined using corresponding distributions of dihedral angles ϕ and φ in the Ramachandran plot. A residue was considered as contributing to α-helices when $-90° < \phi < -35°$ and $-70° < \varphi < -15°$, to β-sheets when $-165° < \phi < -105°$ and $105° < \varphi < 165°$, and to polyproline II structures when $-105° < \phi < -45°$ and $120° < \varphi < 180°$. The randomness of the distribution of residues with a particular secondary structure along the protein chain was analyzed by the probability distribution of clusters containing S successive residues of the same kind. Clustering of similar residues in the peptide chain belongs to the site-percolation problem in one-dimensional systems. In an infinite chain, the probability n_S of finding S successive residues of the same kind in the case of their random (noncorrelated) distribution is[43]

$$n_S = (1-p)^2 p^S, \tag{1}$$

where the occupancy probability p in the case of a biopolymer chain is the fraction of residues with some particular secondary structure. The qualitative shape of the probability distribution n_S in finite chains is similar to that in an infinite chain [Eq. (1)], but the probabilities of clusters with small S are higher in the former case.[44]

The analysis of water clustering in hydration shells of various widths was performed similarly to previous studies.[37,45] A water molecule was considered as belonging to the hydration shell when the shortest distance between its oxygen atom and the heavy atoms of $A\beta_{42}$ did not exceed some value D, which was varied from 4.0 to 5.5 Å. Two water molecules were considered as H bonded when the distance between their oxygens did not exceed 3.35 Å and their pair interaction energy was below −2.7 kcal/mol. At ambient conditions, these criteria yield on average about 3.3 H-bonded neighbors of a water molecule in pure liquid water. To determine the temperature where a spanning H-bonded water network breaks into an ensemble of small clusters via a percolation transition, we used the occurrence probability n_S^w of water clusters consisting of S^w molecules, the probability distribution $P(S^w_{max})$ of the size S^w_{max} of the largest water cluster, and some other properties of the largest water cluster. The distribution n_S^w calculated with excluding the largest water cluster was used to determine the mean cluster size S^w_{mean}. The distribution $P(S^w_{max})$ was used to calculate the probability [spanning probability (SP)] of finding a *spanning* water cluster, which includes most of the molecules in the hydration shell and homogeneously envelops the peptide.

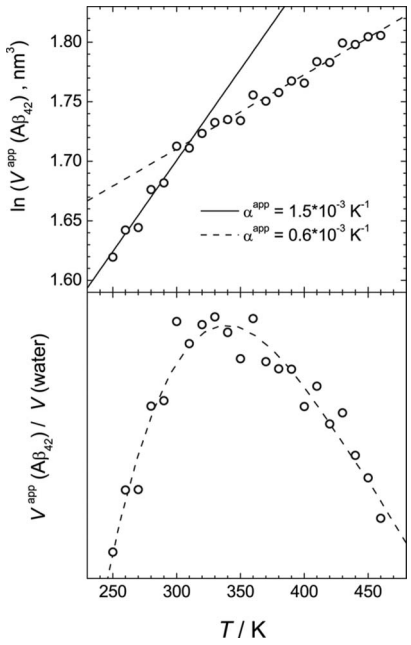

FIG. 1. Upper panel: Temperature dependence of $\ln(V^{app}(A\beta_{42}))$ (circles) and linear fits in two temperature intervals (lines). Lower panel: Ratio of $V^{app}(A\beta_{42})$ to the volume of some arbitrary amount of bulk liquid water. The dashed line is a guide for the eyes only.

III. RESULTS

A. Thermal expansion of protein and hydration water

The temperature dependence of the logarithm of the apparent volume $V^{app}(A\beta_{42})$ of $A\beta_{42}$ is shown in the upper panel of Fig. 1. The derivative $\delta \ln(V)/\delta T$ is equal to the thermal expansion coefficient α. Two linear parts of the temperature dependence of $\ln(V^{app}(A\beta_{42}))$ with a crossover at about 320 K can be distinguished, indicating two quite different values of the thermal expansion coefficient $\alpha^{app}(A\beta_{42})$. Fits to these linear dependencies (solid and dashed lines in the upper panel of Fig. 1) yield $\alpha^{app}(A\beta_{42}) \approx (1.53 \pm 0.13) \times 10^{-3}$ K^{-1} at $T \leq 320$ K and $\alpha^{app}(A\beta_{42}) = (6.23 \pm 0.36) \times 10^{-4}$ K^{-1} at $T > 320$ K. The ratio of the apparent volume of $A\beta_{42}$ to the volume of bulk liquid water (lower panel of Fig. 1) changes with temperature nonmonotonically. Upon heating, the apparent volume of $A\beta_{42}$ increases faster than the water volume being at temperatures below ~340 K and slower above ~340 K. Accordingly, at about 340 K, $\alpha^{app}(A\beta_{42})$ becomes equal to the thermal expansion coefficient of liquid bulk water.

The apparent volume V^{app} of a peptide or any other object in liquid water may be decomposed into two main contributions: the neat or intrinsic volume V^{int} and the contribution ΔV (water), which accounts for a possible difference between the densities of bulk and hydration water. Thus the intrinsic volume of $A\beta_{42}$ may be defined by the following equation:

$$V^{app}(A\beta_{42}) = V^{int}(A\beta_{42}) + \Delta V(\text{water}). \tag{2}$$

The term apparent thus means that contributions due to protein-solvent interactions are included. The term intrinsic means that we are dealing with the bare protein, whose properties cannot be directly measured. Assuming the density of

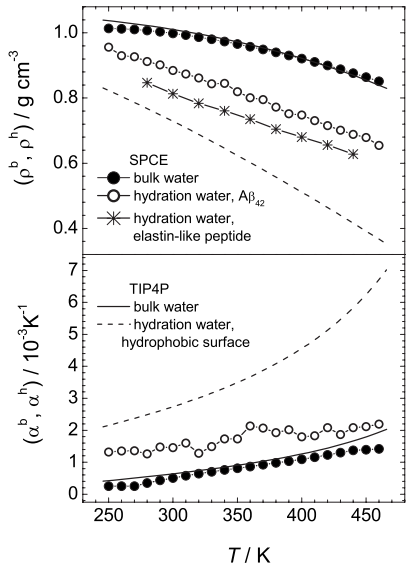

FIG. 2. Temperature dependence of the density (upper panel) and of the thermal expansion coefficient (lower panel) of bulk water and hydration water near Aβ_{42}, near an elastinlike peptide (Ref. 40), and near a paraffinlike surface (Ref. 8) as obtained for two water models, SPCE and TIP4P.

liquid water to be affected by a protein only up to some distance D to its surface, the differential contribution ΔV (water) may be described as

$$\Delta V(\text{water}) = V_D(1 - \rho^h/\rho^b), \tag{3}$$

where ρ^h and ρ^b are the densities of hydration and bulk water, respectively, and V_D is the volume affected by the protein, i.e., the volume of hydration water. As the surface perturbation decays exponentially with the distance to the surface and as this decay is governed by the correlation length of bulk water,[8] the density perturbation beyond the first surface layer may be neglected at ambient temperature. The first minimum in the density profile of liquid water near various surfaces, including biosurfaces, is located at about 4.5 Å.[37] Therefore, it is reasonable to attribute water molecules, whose oxygen are closer than $D \approx 4.5$ Å to the heavy atoms of a biomolecule, to the surface layer. In a first approximation, $V_D = \text{SASA} \cdot (D - 1.5\ \text{Å})$, as half of the typical contact distance between water oxygen and the heavy atoms of the biomolecule (about 1.5 Å) is not accessible for the center of water oxygen. Thus, the density ρ^h of hydration water is equal to $N_w \cdot m_{H_2O}/V_D$, where m_{H_2O} is the mass of a water molecule. Hence, ΔV (water) should be positive if $\rho^b > \rho^h$ and negative otherwise.

The temperature dependencies of the densities ρ^b and ρ^h are compared in the upper panel of Fig. 2. In the whole temperature interval studied, $\rho^h < \rho^b$, which indicates a depletion of the water density near the surface of Aβ_{42}. The density depletion becomes more pronounced upon heating. In fact, such situation is typical of liquid water near hydrophobic surfaces.[8] For comparison, we show the temperature dependence of the water density near a smooth surface, whose hydrophobicity is close to that of paraffin. The water density depletion is markedly stronger in the latter case, in agreement with the fact that the surface of Aβ_{42} is not as hydrophobic as paraffin.

The temperature dependence of the density of bulk and surface water may be described in the framework of the theory of critical behavior.[8–10] When *bulk* liquid is in equilibrium with saturated vapor, its density may be presented as a function of a reduced temperature $\tau = (T_c - T)/T_c$, which measures the distance to the critical temperature T_c,

$$\rho^b = \rho_c[(1 + a_1\tau + a_2\tau^2 + \cdots) + b_1\tau^\beta(1 + b_2\tau^\Delta + \cdots)], \tag{4}$$

with the critical exponents $\beta \approx 0.326$ and $\Delta \approx 0.5$; ρ_c is the critical density, and a_i and b_i are coefficients. Near the surface, the liquid density ρ^h obeys Eq. (4), but with other values of coefficients and critical exponents. In particular, the exponent β near the surface is predicted to be about 0.8.[10] Intrusion of the surface critical behavior into the bulk is governed by the bulk correlation length ξ and extends upon heating. A crossover from the surface critical behavior to the bulk critical behavior occurs when the distance from the surface is about 2ξ.[8,9] The temperature dependence of the liquid density of water and Lennard-Jones fluids in the first (surface) layer follows the laws of surface critical behavior down to the freezing temperature. For water near weakly attractive surfaces, exponent β in the surface layer was found to be close to 1.[8]

Near a hydrophobic surface, the density of liquid water is lower than that in the bulk (see Fig. 2, upper panel). This is caused by a missing neighbor effect, which weakens the intermolecular interaction per fluid molecule near any boundary. This effect appears also in a lowering of the critical density ρ_c near the surface and, accordingly, in a much steeper decrease in liquid density upon heating [large value of the coefficient a_1 in Eq. (4)]. Such behavior is clearly seen for the density of hydration water near the surface of Aβ_{42} as well as near an elastinlike peptide (Fig. 2, upper panel). Accordingly, the thermal expansion coefficient α^h of hydration water is larger than α^b of bulk water. The thermal expansion coefficients α^h obtained by two-point differentiation of the temperature dependence of the density of hydration water near Aβ_{42} and α^b are shown in Fig. 2 (lower panel). The difference $\alpha^h - \alpha^b$ remains positive in the whole temperature range studied, but the two coefficients seem to approach each other upon heating. For the strongly hydrophobic paraffinlike surface, the difference $\alpha^h - \alpha^b$ grows upon heating (see the lower panel of Fig. 2).

The temperature dependence of the logarithm of the inverse density $1/\rho^h$ of hydration water is shown in the upper panel of Fig. 3. The derivative $\delta \ln(1/\rho^h)/\delta T$, which is equal to the thermal expansion coefficient α^h, is not a constant in the temperature interval studied. Mean-square deviations of the dependence $\ln(1/\rho^h)(T)$ from a linear fit decrease by about a factor of 2 if $\ln(1/\rho^h)(T)$ is fitted by two different linear regions at low and high temperatures, respectively. This allows distinguishing of two temperature regimes with slightly different thermal expansion coefficients of the hydration water. At $T \leq 330$ K, $\alpha^h = (1.46 \pm 0.06) \times 10^{-3}$ K^{-1}, whereas at $T > 330$ K, $\alpha^h = (2.00 \pm 0.05) \times 10^{-3}$ K^{-1}. Knowledge of the hydration water density at various temperatures allows calculation of ΔV (water) using Eq. (3) and, subsequently, of $V^{\text{int}}(A\beta_{42})$ using Eq. (2). The temperature dependence of $\ln(V^{\text{int}}(A\beta_{42}))$ is shown in the lower panel of

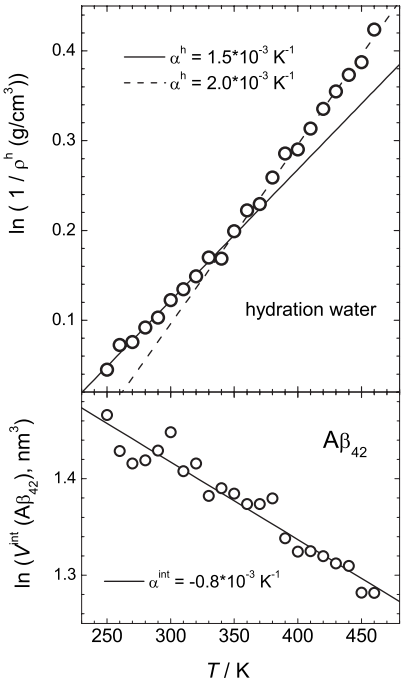

FIG. 3. Upper panel: Temperature dependence of $\ln(1/\rho^h)$ for hydration water of $A\beta_{42}$. Lower panel: Temperature dependence of $\ln(V^{\text{int}}(A\beta_{42}))$, where $V^{\text{int}}(A\beta_{42})$ is the intrinsic volume of $A\beta_{42}$. The slope of each linear fit reflects the thermal expansion coefficient.

Fig. 3. The intrinsic thermal expansion coefficient of $A\beta_{42}$, estimated from the linear approximation of $\ln(V^{\text{int}}(A\beta_{42}))$ in the whole temperature range studied, is *negative*: $\alpha^{\text{int}}(A\beta_{42}) = -(0.80 \pm 0.05) \times 10^{-3}\ \text{K}^{-1}$. The scattering of the data points does not allow a more detailed analysis of the temperature dependence of $\alpha^{\text{int}}(A\beta_{42})$.

B. Conformational behavior of $A\beta_{42}$

The radius of gyration R_{gyr} and SASA of $A\beta_{42}$ decrease upon heating (Fig. 4). Despite the strong scattering of the data points caused by the relatively short simulation runs used (20 ns), the decrease in both R_{gyr} and SASA upon heating is clearly seen. Use of the longer simulation runs for some of the temperatures (see solid circles in Fig. 4) confirms this observation. The radius of gyration R_{gyr} of $A\beta_{42}$ decreases from about 15 to 11 Å upon heating from 280 to 380 K (see the lower panel of Fig. 4). At the lowest and highest temperatures studied, some trend to saturation may be noticed in the temperature dependence of R_{gyr}. Indeed, a sigmoidal curve gives a better description of $R_{\text{gyr}}(T)$ in comparison with a linear fit (mean-square deviations of the data points from the fitted line increase by about 25% in the latter case). A fit of $R_{\text{gyr}}(T)$ by a sigmoidal curve (line in the lower panel of Fig. 4) indicates an inflection point at about 340 K. A quite similar temperature behavior is seen in the SASA of $A\beta_{42}$, and its fit to a sigmoidal function yields an inflection point at about 320 K (see the upper panel of Fig. 4). The joint probability distribution of R_{gyr} and SASA of $A\beta_{42}$ allows an analysis of the correlation between these two parameters (distributions for the lowest and highest temperatures studied are shown in Fig. 5). Such a correlation is practically absent for the low-temperature conformation of $A\beta_{42}$, which

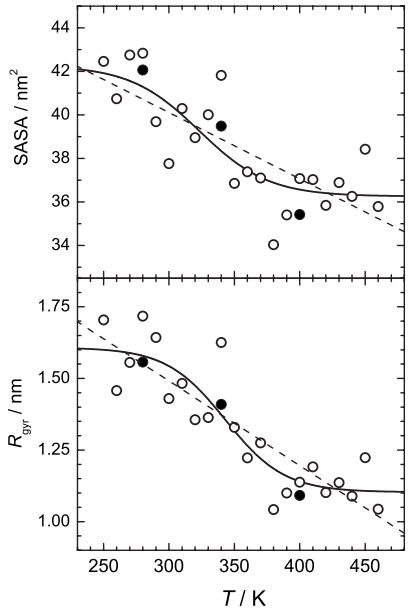

FIG. 4. Temperature dependence of the radius of gyration R_{gyr} and SASA of $A\beta_{42}$. Fits to a sigmoidal and linear dependence are shown by solid and dashed lines, respectively. Solid circles show the data points obtained in 40 ns simulation runs.

is characteristic of an extended chain. A clear correlation between SASA and R_{gyr} is found for the high-temperature conformation of $A\beta_{42}$. Taking into account that SASA $\sim (R_{\text{gyr}})^2$ for spherical objects and SASA $\sim R_{\text{gyr}}$ for elongated ellipsoids or cylinders, the shape of the high-temperature conformation of $A\beta_{42}$ appears to be essentially spherical. An analysis of such kind reveals that $A\beta_{42}$ undergoes a transition from an extended chainlike conformation to a more compact coil conformation upon heating. The midpoint of this transition is approximately at 320–340 K.

The temperature dependence of the fraction of residues with some particular secondary structure defined using their dihedral angles is shown in the upper panel of Fig. 6. The fraction p of residues with dihedral angles characteristic of α-helices decreases three times upon heating from 260 to

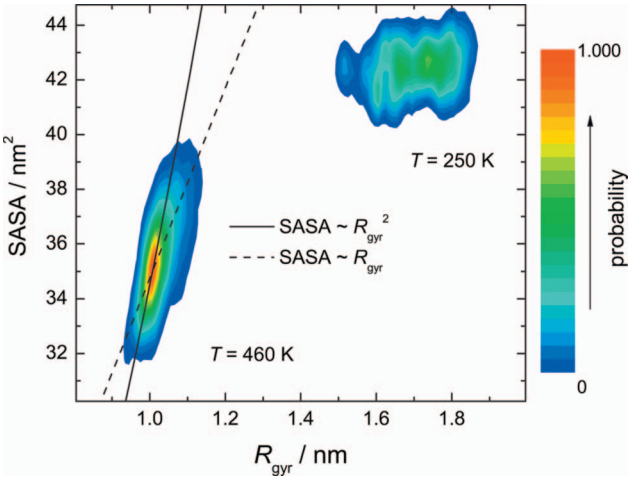

FIG. 5. (Color) Joint probability distribution of the SASA and radius of gyration of $A\beta_{42}$ at the lowest and highest temperatures studied. The color scale on the right-hand side indicates changes in the occurrence probability.

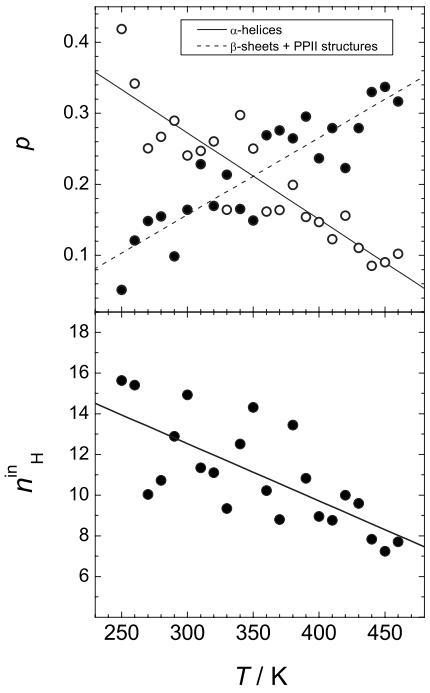

FIG. 6. Content p of the residues with particular secondary structure (upper panel) and average number n_H^{in} of intrapeptide H bonds. Linear fits are shown by lines.

about 430 K. In parallel, the corresponding values of p for β-sheets and polyproline II structures (which are approximately equally populated) increase by about a factor of 3 upon heating. The probability distributions n_S of the clusters of residues with like secondary structures are shown in Fig. 7 together with the random distributions expected for an infinite chain with the same content p. The distribution n_S of β-sheets is close to the random one at all temperatures studied. Upward deviations of n_S from Eq. (1) at small S are due to the finite size effect that facilitates the formation of

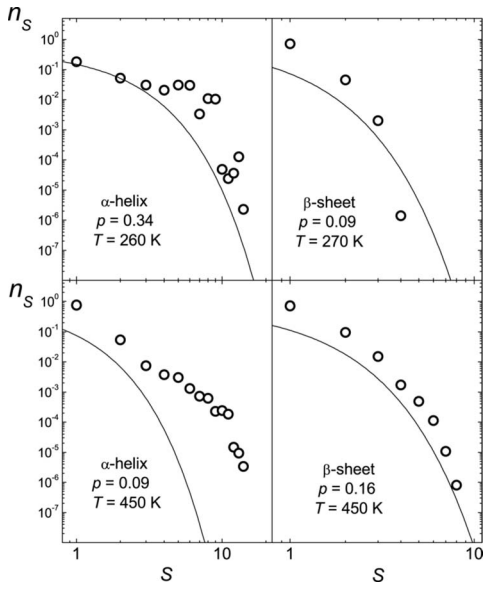

FIG. 7. Probability n_S of finding S successive residues with the same secondary structure. Lines show n_S for a random distribution of residues in an infinite chain [Eq. (1)] with the same content p of residues with like structure.

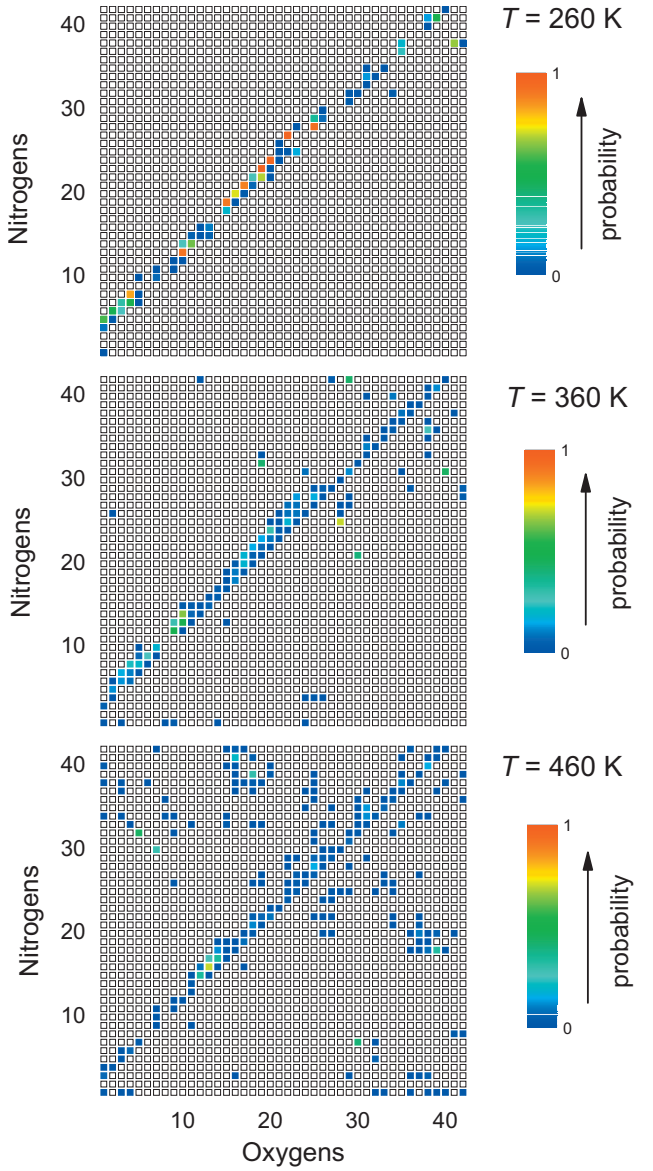

FIG. 8. (Color) Map of intrapeptide N–H···O hydrogen bonds of Aβ_{42}. The color scale on the right-hand side indicates changes in the occurrence probability.

smaller clusters.[44] Similar distributions n_S were found for residues attributed to the polyproline II structure (not shown). For α-helices, the distributions n_S evidence a correlation between successive residues: there are clusters of α-helices with large S values (up to $S=14$), which do not appear for β-sheets and polyprolines, where S does not exceed 4 at the same content p (see Fig. 7). At all temperatures, the distribution n_S for α-helices deviates upward from Eq. (1) at large S, supporting the trend toward cooperative "condensation" of residues with α-helical dihedral angles.

The maps, which show the probability distribution of intrapeptide N–H···O bonds between various residues (Fig. 8), give valuable insight into the secondary structure of Aβ_{42}. At low temperatures, most of the intrapeptide H bonds are formed between residues i and $(i+\Delta i)$, with $\Delta i=2$, 3, 4, or 5, which are characteristic of various helices, loops, and turns. Figure 8 evidences a high probability of such intrapeptide H bonds along four diagonal lines at $T=260$ K, which

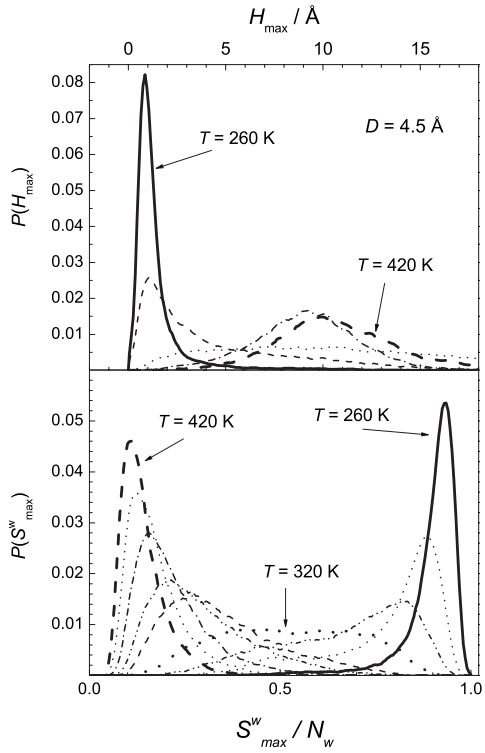

FIG. 9. Upper panel: Probability distribution $P(H_{\max})$ of the distance $H_{\max}$ between the center of mass of Aβ_{42} and the center of mass of the largest hydration water cluster. Lower panel: Probability distribution $P(S_{\max})$ of the size $S_{\max}$ of the largest water cluster, normalized by the average number N_w of water molecules in the hydration shell of width D=4.5 Å.

agrees qualitatively with a higher content of α-helices at low temperatures (Fig. 6, upper panel). Upon heating, the average number of intrapeptide H bonds decreases noticeably (see the lower panel in Fig. 6). This occurs mainly due to the break of H bonds with Δi=2, 3, 4, or 5 (not shown). Accordingly, the fraction of H bonds with $\Delta i > 5$, which corresponds to β-sheets and also to irregular H bonds between distant residues, increases with temperature (Fig. 8). Temperature-induced changes in the secondary structure of Aβ_{42} are rather gradual and do not show an indication of a conformational transition.

C. Thermal break of spanning water network

To study the relation between the conformational properties of Aβ_{42} and the structure of hydration water, we have analyzed the clustering of hydration water at all temperatures studied. Various cluster properties were calculated in order to detect the thermal break of a spanning water network (see Sec. II). Some results, obtained for clustering of water molecules with their oxygen located within the hydration shell of a D=4.5 Å width, are shown in Figs. 9–13. In particular, the probability distributions $P(H_{\max})$ of the distance $H_{\max}$ between the centers of mass of Aβ_{42} and of the largest water cluster in its hydration shell are shown in the upper panel of Fig. 9. At low temperatures, $H_{\max}$ is close to zero, indicating a homogeneous coverage of Aβ_{42} by a H-bonded network of hydration water. At high temperatures, $H_{\max}$ is comparable with the radius of gyration of Aβ_{42}, and a spanning network of hydration water is absent. The transition between these

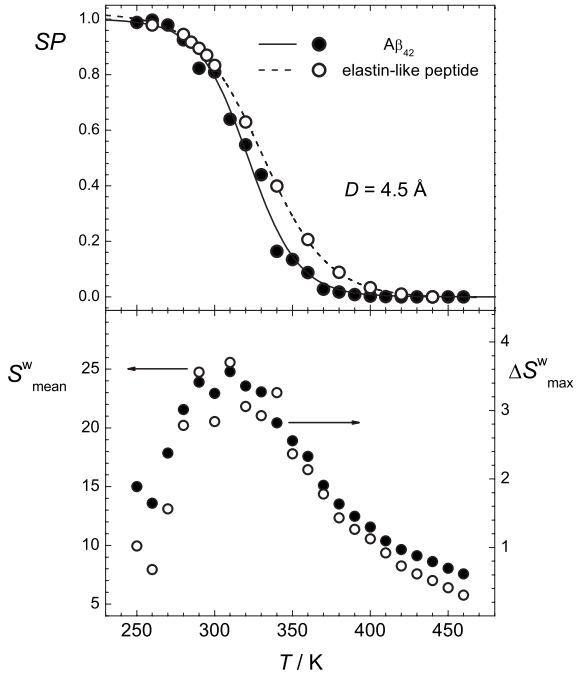

FIG. 10. Upper panel: Temperature dependence of the SP in the hydration shell of width D=4.5 Å at the surface of Aβ_{42} and of an elastinlike peptide (Ref. 40). Lower panel: Temperature dependence of the mean cluster size S^w_{mean} and of the width $\Delta S^w_{\max}$ of the probability distribution $P(S^w_{\max})$ in the hydration shell of Aβ_{42}.

two qualitatively different states of hydration water is a percolation transition from a state with a majority of molecules in one spanning network to an ensemble of small clusters. The evolution of the probability distribution $P(S^w_{\max})$ of the size $S^w_{\max}$ of the largest cluster of hydration water upon heating, shown in the lower panel of Fig. 9, is typical of the percolation transition in finite systems. The largest water cluster includes the majority of molecules ($S^w_{\max}/N_w$ is close to 1) at low temperatures (T<320 K) and the minority ($S^w_{\max}/N_w$ approaches 0) at higher temperatures.

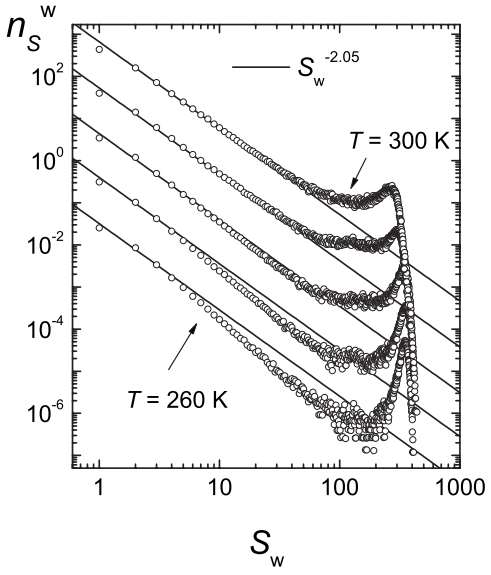

FIG. 11. Cluster size distributions n^w_S for water in the hydration shell of Aβ_{42} of width D=4.5 Å at temperatures T=260, 270, 280, 290, and 300 K in the vicinity of the percolation transition. The distributions are shifted by one order of magnitude, starting from the bottom.

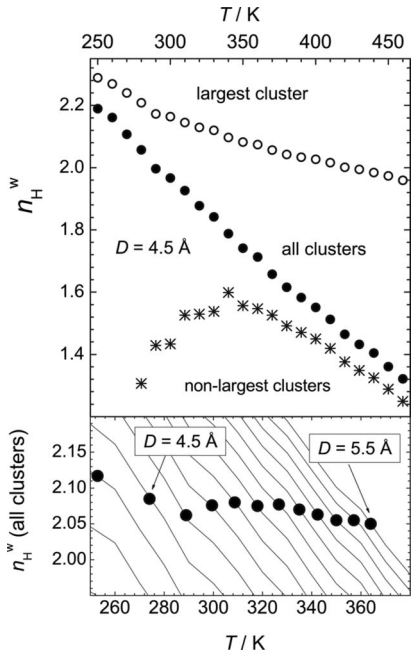

FIG. 12. Upper panel: Temperature dependence of the average number n_H^w of H-bonded neighbors of a water molecule in various clusters. Lower panel: Temperature dependence of n_H^w for all clusters (lines) and location of the percolation transition (solid circles) in the water shells of various widths D.

The SP, which is the probability of observing a spanning cluster of hydration water in an arbitrarily chosen configuration, can be approximately estimated as an integral of $P(S_{max}^w)$ over $S_{max}^w/N_w > 0.5$.[46] The temperature dependence of SP, shown in the upper panel of Fig. 10, may be well fitted to a sigmoid with an inflection point (SP=50%) at about 320 K. This temperature marks the midpoint of the percolation transition, where spanning and nonspanning largest water clusters exist with equal probabilities. Percolation theory reveals that SP as well as the location of its inflection point are size-dependent properties, whereas a *true* percolation threshold marks the location of the percolation transition in an infinite system. Such a true percolation threshold corresponds to some particular value of SP, which depends on the definition of the spanning cluster, the system dimensionality, but depends only slightly on the system size.[47] For quasi-two-dimensional (2D) percolation on the surface of a finite object, SP is about 95% at the true percolation threshold.[46] Hence, a true percolation threshold of hydration water in the shell of a width of $D=4.5$ Å is at about 280–290 K. This agrees with the temperature evolution of the cluster size distribution n_S^w (Fig. 11). The distribution n_S^w at the percolation threshold should follow the universal power law for 2D percolation (lines in Fig. 11) in the widest range of cluster sizes S^w. As can be seen in Fig. 11, this indeed happens at some temperature between 280 and 290 K.

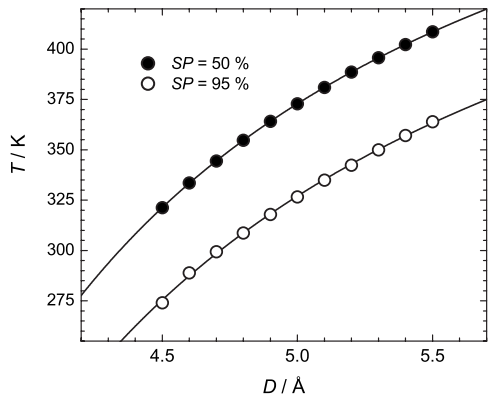

FIG. 13. Temperatures corresponding to the SP=50% and SP=95% in water shells of various widths D. Fits to Eq. (5) are shown by lines.

The temperature dependence of the mean size S_{mean}^w of water clusters in the hydration shell, calculated without the largest cluster, is shown in the lower panel of Fig. 10. As expected, this dependence passes through a maximum when approaching the true percolation threshold upon cooling. The maximum of S_{mean}^w occurs close to the midpoint of the percolation transition. Approximately at the same temperature, the probability distribution of the largest cluster $P(S_{max}^w)$ is the widest (see Fig. 9). The width ΔS_{max}^w of this distribution can be estimated as a standard deviation of S_{max}^w normalized by $N_w^{0.5}$.[39] The temperature dependence of ΔS_{max}^w shows a maximum at about 310–320 K (Fig. 10). So, the temperature dependencies of both S_{mean}^w and ΔS_{max}^w evidence the largest fluctuations of hydrogen-bonded water networks in the hydration shell at about 310 K. The average number n_H^w of H bonds, which one water molecule forms in the hydration shell, is about 2.0–2.1 at the true percolation threshold. Please note that this value is rather universal[45] for smooth surfaces and biomolecules, and it is not sensitive to the choice of the width of the hydration shell D around Aβ_{42}, as can be seen from the lower panel of Fig. 12. The value of n_H^w, calculated for water molecules in all clusters excluding the largest one, passes through the maximum at about 320 K, which is close to the temperature where the mean cluster size S_{mean}^w has a maximum. n_H^w calculated within the largest water cluster only has a rather weak temperature dependence without noticeable peculiarities.

The results presented above describe the water clustering in the first water monolayer, which includes water molecules in the shell of a 4.5 Å width. Obviously, a spanning water network in thicker layers should be more stable with respect to heating. The temperatures, where SP=50% (midpoint of the percolation transition) and SP=95% (true percolation transition), are shown in Fig. 13 as a function of the width D of the hydration shell analyzed. Both characteristic temperatures increase with increasing D. Contrary to the water monolayer, the width of the adsorbed water bilayer depends on the kind of the adsorbing surface: D is about 7.5 Å for smooth surfaces and should exceed at least 6.5 Å in the presence of water-surface H bonds. Extrapolation of the dependencies in Fig. 13 to higher values of D indicates that the spanning water network exists in a water bilayer in a wide range of biologically relevant temperatures. Being in equilibrium with saturated vapor, the spanning water network in the limit $D \to \infty$ should break at the liquid-vapor critical point, which is a point of the three-dimensional percolation transition of physical clusters.[48] Due to the relatively low temperatures used in our constant-pressure simulations, the liquid water density is very close to its value at the liquid-vapor coexistence curve. Accordingly, the dependence of the tem-

perature T_p, corresponding to some chosen value of SP, on the width D can be fitted by an empirical equation of the form

$$T_p = T_c^* - A/(D - D_c), \tag{5}$$

where D_c is a minimal possible thickness of a percolating water shell, A is a constant, and T_c^* is an apparent critical temperature. The fit of the dependence for SP=50% to Eq. (5) gives $T_c^* \approx 604$ K and $D_c \approx 2.3$ Å. The first value is just slightly below the critical temperature of SPCE water, estimated from the simulated liquid-vapor coexistence curve.[49] Notably, the value of the SP=50% is close to the critical value of the wrapping probability of finding an infinite cluster in three-dimensional systems, which is about 44%.[47]

IV. DISCUSSION

By taking into account the different temperature dependencies of the water density in the bulk and in hydration shell, we determined the temperature dependence of the intrinsic volume V^{int} of Aβ_{42} and its expansion coefficient α^{int}. To the best of our knowledge, this is the first estimation of an intrinsic thermal expansion coefficient of a biomolecule in water. In crystals, α of biomolecules is small ($\sim 10^{-4}$ K^{-1}) and positive.[50] However, Aβ_{42} in solution shows a negative intrinsic expansion coefficient (Fig. 3), which means that it contracts and becomes more densely packed upon heating. Moreover, our preliminary results show that also the elastinlike peptide, studied in Ref. 40, has a negative α^{int}, whose absolute value is about two times larger than α^{int} of Aβ_{42}.

A negative expansion coefficient of a biomolecule may be related to the entropic character of its elasticity. Generally, noncrystalline (amorphous or disordered) macromolecular and biomolecular[51–55] substances show some kind of rubberlike elastic behavior at temperatures well above their glass temperature.[56] The glass temperature for dry biomolecules is very high, and they are in the glassy state at ambient conditions. Upon hydration, the glass temperature drastically decreases, and the complete dynamics of biomolecules is restored when they are covered by about 1 monolayer of hydration water.[7] Rubber elastic behavior originates from a decrease in entropy upon elongation of a polymer chain due to the decreasing number of available configurations, and it is observed above the θ-point of a polymer solution. The increase in entropy upon heating enhances the contractive forces, thus leading to a negative expansion coefficient of rubber elastic bodies. It was shown recently[40] that a single elastinlike peptide in water exhibits a distribution of the end-to-end distances close to one of an ideal random chain with a purely entropic elasticity. This explains the negative thermal expansion coefficient of elastinlike peptides in water.

The anomalous (negative) intrinsic expansivity of a biomolecule correlates with a decrease in intramolecular H bonding upon heating. Indeed, the average—irrespective of accompanying conformational changes—number of intrapeptide H bonds of Aβ_{42} decreases from about 15 at 250 K to about 8 at 460 K (see the lower panel in Fig. 6). A similar behavior is observed for the elastinlike peptide, where this number decreases from about 7 to 5.5 upon heating from 280 to 440 K.[40] We may assume that intrapeptide H bonds of Aβ_{42} prevent close packing of the peptide chain, whereas a decrease in the number of such bonds should help to pack the peptide more tightly. As a consequence, also the defect or void volume will be diminished at higher temperatures. A similar process occurs in supercooled water, where the collapse of more open structures upon heating is strong enough to overcome conventional thermal expansion and to provide a negative intrinsic thermal expansion coefficient.[57]

The obtained temperature dependence of the apparent thermal expansion coefficient α^{app}(Aβ_{42}) (Fig. 1) is quite similar to the dependencies of $\alpha^{\text{app}}(T)$ obtained for various biomolecules experimentally:[2–5] α^{app} is positive at low temperatures and decreases upon heating. Our results indicate that such behavior of α^{app} for the system studied here reflects mainly the specific temperature behavior of "water defects," which account for the different temperature dependencies of the volumetric properties of bulk and hydration water [Eq. (2)]. Large positive values of α^{app} at low temperatures are due to the fact that the thermal expansion coefficient of hydration water essentially exceeds the bulk value. This difference decreases with temperature, as the thermal expansion coefficients of bulk and hydration water approach each other (Fig. 2). However, this does not explain the noticeable change in the apparent volumetric properties in a rather narrow temperature interval near 320 K (see the upper panel in Fig. 1). This behavior may originate from the specific intrinsic properties of Aβ_{42} and/or from the specific properties of the hydration water.

The Aβ_{42} peptide exhibits an essentially disordered conformational structure at all temperatures studied. Residues with like secondary structures are distributed almost randomly along the peptide chain (Fig. 7), and only for residues having α-helical dihedral angles, some trend toward condensation can be noticed. The absence of a well-defined conformation of Aβ_{42} in water was seen in experiments[14,17,19] as well as in other simulation studies of Aβ_{42}, where quite different force fields and starting configurations were used.[17,26–31] Quite similarly, essentially disordered conformations of other amyloid-β peptides and their fragments in water are seen both in experiments[14,22,58] and in simulations.[32–35] Upon heating, Aβ_{42} loses elements of the secondary structure, characterized by intrapeptide H bonds with $\Delta i = 2$, 3, 4, and 5 (such as α-helices), and adopts β-like conformations (Figs. 7 and 8). The same trend is seen in the experimental studies of the amyloid β-peptides in water[21] as well as in the simulation studies of a simplified model of the Aβ_{42} peptide in implicit water.[36]

The geometrical analysis evidences that the Aβ_{42} peptide is essentially an extended chain at low temperatures and is a relatively compact coil at higher temperatures. Such temperature behavior is opposite to that of elastinlike peptides.[40] Note that despite these qualitative differences, both peptides show a negative thermal expansivity. The obtained simulation results allow us to suggest that the absence of a well-defined conformation as well as the decreasing number of intrapeptide H bonds upon heating may be the key factors that cause the negative thermal expansivity of these peptides.

The change in the apparent volumetric properties of the

$A\beta_{42}$ peptide at about 320 K may originate from a temperature-induced conformational transition. No clear evidences of such a transition can be seen from the behavior of the secondary structure content (Fig. 6), and only a rather gradual transition with a midpoint at about 320–340 K is observed in the behavior of geometrical parameters (Fig. 4). Hence, we may expect that the volumetric properties are more sensitive to the temperature-induced conformational changes of such a disordered peptide as $A\beta_{42}$. These changes are not clearly seen in the temperature dependence of the intrinsic volume of $A\beta_{42}$ (lower panel in Fig. 3) due to the strong scattering of the data points, and further studies are necessary to clarify the sensitivity of the intrinsic volume of a peptide to its conformational changes. However, slight changes in the expansivity of hydration water at about 330 K may simply reflect the fact that the peptide surface becomes slightly more hydrophobic above this temperature due to some minor conformational changes. The decrease in the solubility of $A\beta_{42}$ upon heating corroborates this idea. If the latter explanation is correct, we may conclude that at least for disordered peptides, the thermal expansivity of hydration water may be a more adequate order parameter of the conformational transition than, for example, the radius of gyration or the secondary structure content.

Alternatively, the change in the apparent volumetric properties of the $A\beta_{42}$ peptide at about 320 K may originate solely from the intrinsic temperature behavior of the hydration water. Below this temperature, the hydration water forms an extended H-bonded network, which includes most of the water molecules in the hydration shell, whereas at higher temperatures, only small H-bonded clusters are present in the hydration shell. The percolation transition between these two qualitatively different states occurs in a rather narrow temperature interval (Fig. 10). Hence, the thermal expansion of hydration water may differ in these two states, being higher for the more disordered one. To support this explanation, the thermal expansion coefficient of hydration water should be studied in detail for surfaces with various strengths of the temperature-independent water-wall interaction.

Interestingly, the qualitative changes in the conformational properties of elastinlike peptides[40] and in the apparent volumetric properties of the $A\beta_{42}$ peptide occur when the spanning network of their hydration water breaks upon heating. As can be seen from the upper panel of Fig. 10, the temperatures of this break are close for these two peptides. The difference in the temperature dependence of the SP appears in a small ($\sim$10 K) shift in the inflection point and in a notable difference in the sigmoid width, which is naturally attributed to the difference in peptide sizes (the SASA of $A\beta_{42}$ is about two times larger). The similarity of the behaviors of hydration water at the surfaces of the two different peptides may originate from a rather close level of the hydrophobicity of their surfaces (approximately 50% hydrophobic residues in both cases). This can be seen in the upper panel of Fig. 2, where the densities of the hydration water of these two peptides are compared: the surface of the elastinlike peptide is only slightly more hydrophobic. We may assume that—owing to the strong coupling between the peptide and hydration water[59]—the thermal break of the spanning network of hydration water provokes (or speeds up) conformational changes of a peptide. The character of these changes seems to be governed by the chemical nature of the peptide. Further studies are needed to clarify the relation between the peptide structure (amino acid sequence) and the temperature of the percolation transition of hydration water on its surface. This includes both the effects of peptide hydrophilicity/hydrophobicity on water percolation and the effect of water clustering in the hydration shell on the conformational and volumetric properties of the peptide.

ACKNOWLEDGMENTS

Financial support from the DFG and the Center for Applied Chemical Genomics (ZACG, Dortmund) is gratefully acknowledged.

[1] T. V. Chalikian, Annu. Rev. Biophys. Biomol. Struct. **32**, 207 (2003).
[2] H. Seemann, R. Winter, and C. A. Royer, J. Mol. Biol. **307**, 1091 (2001).
[3] R. Ravindra, C. Royer, and R. Winter, Phys. Chem. Chem. Phys. **6**, 1952 (2004).
[4] L. Mitra, N. Smolin, R. Ravindra, C. Royer, and R. Winter, Phys. Chem. Chem. Phys. **8**, 1249 (2006).
[5] C. Nicolini, R. Ravindra, B. Ludolph, and R. Winter, Biophys. J. **86**, 1385 (2004).
[6] M. Hiebl and R. Maksymiw, Biopolymers **31**, 161 (1991).
[7] I. Brovchenko and A. Oleinikova, *Interfacial and Confined Water* (Elsevier, Amsterdam, 2008).
[8] I. Brovchenko, A. Geiger, and A. Oleinikova, J. Phys.: Condens. Matter **16**, S5345 (2004).
[9] I. Brovchenko, A. Geiger, and A. Oleinikova, Eur. Phys. J. B **44**, 345 (2005).
[10] K. Binder, in *Phase Transitions and Critical Phenomena*, edited by C. Domb and J. L. Lebowitz (Academic, London, 1983), Vol. 8, p. 1.
[11] F. Chiti and C. M. Dobson, Annu. Rev. Biochem. **75**, 333 (2006).
[12] C. Haass and D. J. Selkoe, Nat. Rev. Mol. Cell Biol. **8**, 101 (2007).
[13] C. Barrow and M. Zagorski, Science **253**, 179 (1991).
[14] C. J. Barrow, A. Yasuda, P. T. M. Kenny, and M. G. Zagorski, J. Mol. Biol. **225**, 1075 (1992).
[15] O. Crescenzi, S. Tomaselli, R. Guerrini, S. Salvadori, A. M. D'Ursi, P. A. Temussi, and D. Picone, Eur. J. Biochem. **269**, 5642 (2002).
[16] Y. Fezoui and D. B. Teplow, J. Biol. Chem. **277**, 36948 (2002).
[17] S. Tomaselli, V. Esposito, P. Vangone, N. A. J. van Nuland, A. M. J. J. Bonvin, R. Guerrini, T. Tancredi, P. A. Temussi, and D. Picone, ChemBioChem **7**, 257 (2006).
[18] J. D. Harper and P. T. Lansbury, Annu. Rev. Biochem. **66**, 385 (1997).
[19] R. Riek, P. Guntert, H. Dobeli, B. Wipf, and K. Wuthrich, Eur. J. Biochem. **268**, 5930 (2001).
[20] L. C. Serpell, Biochim. Biophys. Acta **1502**, 16 (2000).
[21] O. Gursky and S. Aleshkov, Biochim. Biophys. Acta **1476**, 93 (2000).
[22] S. Zhang, K. Iwata, M. J. Lachenmann, J. W. Peng, S. Li, E. R. Stimson, Y. a. Lu, A. M. Felix, J. E. Maggio, and J. P. Lee, J. Struct. Biol. **130**, 130 (2000).
[23] M. G. Zagorski and C. J. Barrow, Biochemistry **31**, 5621 (1992).
[24] E. Terzi, G. Holzemann, and J. Seelig, Biochemistry **33**, 1345 (1994).
[25] J. Kim, J. E. Kim, and M. Lee, Bull. Korean Chem. Soc. **25**, 601 (2004).
[26] A. Baumketner, S. L. Bernstein, T. Wyttenbach, G. Bitan, D. B. Teplow, M. T. Bowers, and J.-E. Shea, Protein Sci. **15**, 420 (2006).
[27] L. Triguero, R. Singh, and R. Prabhakar, J. Phys. Chem. B **112**, 2159 (2008).
[28] L. Triguero, R. Singh, and R. Prabhakar, J. Phys. Chem. B **112**, 7123 (2008).
[29] L. Shen, H.-F. Ji, and H.-Y. Zhang, J. Phys. Chem. B **112**, 3164 (2008).
[30] E. Nordling, Y. Kallberg, J. Johansson, and B. Persson, J. Comput.-Aided Mol. Des. **22**, 53 (2008).
[31] D. Raffa and A. Rauk, J. Phys. Chem. B **111**, 3789 (2007).
[32] Y. Xu, J. Shen, X. Luo, W. Zhu, K. Chen, J. Ma, and H. Jiang, Proc. Natl. Acad. Sci. U.S.A. **102**, 5403 (2005).
[33] G. Wei and J.-E. Shea, Biophys. J. **91**, 1638 (2006).

[34] J. Ikebe, N. Kamiya, J.-I. Ito, H. Shindo, and J. Higo, Protein Sci. **16**, 1596 (2007).
[35] P. Anand, F. S. Nandel, and U. H. E. Hansmann, J. Chem. Phys. **128**, 165102 (2008).
[36] A. R. Lam, B. Urbanc, J. M. Borreguero, N. D. Lazoy, D. B. Teplowy, and H. E. Stanley, BIOCOMP'06 Proceedings, 2006 (unpublished).
[37] I. Brovchenko, A. Krukau, N. Smolin, A. Oleinikova, A. Geiger, and R. Winter, J. Chem. Phys. **123**, 224905 (2005).
[38] I. Brovchenko, A. Krukau, A. Oleinikova, and A. K. Mazur, Phys. Rev. Lett. **97**, 137801 (2006).
[39] I. Brovchenko, A. Krukau, A. Oleinikova, and A. K. Mazur, J. Phys. Chem. B **111**, 3258 (2007).
[40] A. Krukau, I. Brovchenko, and A. Geiger, Biomacromolecules **8**, 2196 (2007).
[41] E. Lindahl, B. Hess, and D. van der Spoel, J. Mol. Model. **7**, 306 (2001).
[42] W. Jorgensen, D. Maxwell, and J. Tirado-Rives, J. Am. Chem. Soc. **118**, 11225 (1996).
[43] P. J. Reynolds, H. E. Stanley, and W. Klein, J. Phys. A **10**, L203 (1977).
[44] K. R. Bauchspiess, Z. Phys. B **37**, 333 (1979).
[45] A. Oleinikova, I. Brovchenko, N. Smolin, A. Krukau, A. Geiger, and R. Winter, Phys. Rev. Lett. **95**, 247802 (2005).
[46] A. Oleinikova and I. Brovchenko, Mol. Phys. **104**, 3841 (2006).
[47] J. Skvor, I. Nezbeda, I. Brovchenko, and A. Oleinikova, Phys. Rev. Lett. **99**, 127801 (2007).
[48] A. Coniglio and W. Klein, J. Phys. A **13**, 2775 (1980).
[49] I. Brovchenko, A. Geiger, and A. Oleinikova, J. Chem. Phys. **123**, 044515 (2005).
[50] H. Frauenfelder, H. Hartmann, M. Karplus, I. D. Kuntz Jr., J. Kuriyan, F. Parak, G. A. Petsko, D. Ringe, R. F. Tilton Jr., M. L. Connolly, and N. Max, Biochemistry **26**, 254 (1987).
[51] C. A. J. Hoeve and P. J. Flory, J. Am. Chem. Soc. **80**, 6523 (1958).
[52] P. J. Flory and O. K. Spurr, J. Am. Chem. Soc. **83**, 1308 (1961).
[53] A. Nakajima and H. A. Scheraga, J. Am. Chem. Soc. **83**, 1575 (1961).
[54] A. Nakajima and H. A. Scheraga, J. Am. Chem. Soc. **83**, 1585 (1961).
[55] G. Loeb and H. A. Scheraga, J. Am. Chem. Soc. **84**, 134 (1962).
[56] L. Mandelkern, Annu. Rev. Phys. Chem. **15**, 421 (1964).
[57] P. G. Debenedetti, J. Phys.: Condens. Matter **15**, R1669 (2003).
[58] J. Danielsson, J. Jarvet, P. Damberg, and A. Graslund, FEBS J. **272**, 3938 (2005).
[59] P. Ball, Chem. Rev. (Washington, D.C.) **108**, 74 (2008).